

Biochimica et Biophysica Acta, 466 (1977) 209–230

© Elsevier/North-Holland Biomedical Press

BBA 77680

THE MOLECULAR ORGANIZATION OF ASYMMETRIC LIPID BILAYERS AND LIPID-PEPTIDE COMPLEXES

T.J. McINTOSH, R.C. WALDBILLIG * and J.D. ROBERTSON

Department of Anatomy, Duke University School of Medicine, Durham, N.C. 27710 (U.S.A.)

(Received October 28th, 1976)

Summary

Oriented fatty acid bilayers with asymmetric distributions of lipid head group types, hydrocarbon chain lengths, and associated polypeptides have been analyzed by a combined use of high resolution electron microscopy and X-ray diffraction techniques. The exclusion of fixatives, stains, and embedding materials has made it possible to relate unequivocally microscopic images to molecular composition. The ultrastructure of asymmetric bilayers has been determined by a novel analysis in which one half of the bilayer serves as a structural reference for the entire bilayer. Absolute electron density profiles at 7 Å resolution have been computed for bilayers formed from long and short chain length lipids either segregated to opposite sides or mixed together in both sides of the bilayer. The data indicate that the two lipids self organize in a specific paired configuration. Detailed analysis of bilayers associated with poly-L-lysine shows that although this hydrophilic peptide resides near the lipid head group region, its presence alters the arrangement of the bilayer hydrocarbon chains.

Introduction

It has been known for a number of years that many biological membranes are structurally asymmetric. This asymmetry has been shown by electron microscopy [1–3], X-ray diffraction [2,4,5], chemical techniques [6–12] and, most recently, by a combination of freeze-fracture and direct chemical analysis [13]. The segregation of particular chemical groups to either the inner or outer side of the bilayer is reflected in both the functional and structural attributes of membranes [14–16].

Model membrane studies have also indicated that some membrane com-

* Present address: Department of Physiology and Biophysics, University of Texas Medical Branch, Galveston, Texas 77550 (U.S.A.).

ponents may spontaneously organize in an asymmetric structure [17]. Asymmetric bimolecular lipid membranes have been produced from interfacial films for electrophysiological studies [18–20] and these planar membranes have been shown by electrical measurements [21] to be relatively stable.

Although biological membranes are asymmetric, most ultrastructural studies of model systems have been performed with symmetric lipid bilayers [22–25]. We have recently demonstrated that well oriented asymmetric lipid bilayers having controlled chemical distributions could be formed from monolayers for analysis by high resolution electron microscopic [26] and X-ray diffraction techniques [27]. In this study we describe the molecular organization of model membranes having a well defined asymmetric distribution of lipids and polypeptides. Electron microscopic images of unfixed, unembedded, and unstained asymmetric bilayers are correlated with 7 Å resolution absolute electron density profiles of the same bilayers derived from X-ray diffraction analysis.

Methods

Multilayers

Condensed lipid monolayers were formed into Langmuir-Blodgett multilayers [28,29] as described previously [26]. Either behenic acid ($C_{22}H_{44}O_2$) or palmitic acid ($C_{16}H_{32}O_2$) was spread at the air/water interface and compressed to an area/molecule of approximately 20 \AA^2 (at 22°C). Unsaponified monolayers were formed on subsolutions of glass distilled water while saponified films were formed on 10 mM alkaline earth chloride solutions (pH 9). Fatty acid-polypeptide monolayers were formed by spreading the lipid on subsolutions containing 20 mg/l of poly-L-lysine in pure water.

The manner in which interfacial monolayers were transferred from the subsolution and onto either epoxy or glass plates has been described in detail earlier (see Fig. 1, ref. 26). In brief, monolayers were made to join together by vertically dipping the support down and up through the air/water interface, resulting in the Y-type [29] transfer of two monolayers having their head groups directed towards each other. Bilayers were assembled in a planned sequence by repeatedly dipping the support through the monolayer.

Asymmetric bilayers were formed by dipping the support downward and upward through one kind of monolayer and then downward and upward through a second kind of monolayer [26,30]. This alternation was repeated a predetermined number of times to form stacks of chemically asymmetric bilayers. It is important to recognize that while the two types of lipid monolayers are apposed tail to tail, identical head groups are always abutted in adjacent bilayers (see Fig. 1). Thus, within the multilayer there is a center of symmetry between adjacent bilayers. This fact is vital to the X-ray diffraction analysis of the structure.

Electron microscopy

The methods of preparing multilayer specimens for microscopic examination have been described in detail previously [26]. Similar procedures were first used by Schidlovsky [31]. Bilayers were deposited in pre-determined sequences upon the surface of an epoxy wafer and the unfixed and unembedded wafer

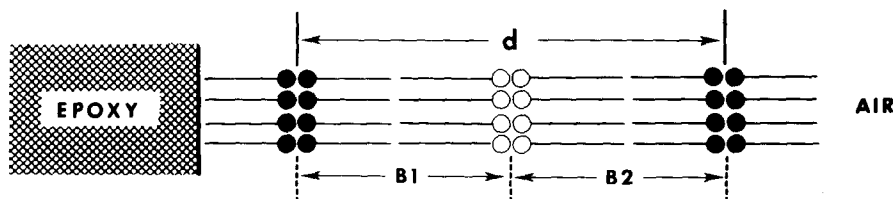


Fig. 1. Schematic diagram showing the molecular arrangement of asymmetric bilayers formed by alternately dipping an epoxy wafer through two different lipid monolayers. After three down and up dipping cycles two asymmetric bilayers, labelled B1 and B2, have been formed. For X-ray diffraction experiments, 20–50 asymmetric bilayers are stacked on the epoxy wafer, and the repeat period, labelled d , contains two asymmetric bilayers with a center of symmetry between them.

was placed directly into an ultramicrotome for thin sectioning. The trimmed wafer was oriented so that the horizontal planes of the bilayer were perpendicular to the cutting edge of a diamond knife (i.e. long axis of hydrocarbon chains parallel to the knife edge) and transverse sections approximately 500 Å thick were cut onto distilled water. These sections were directly examined with a Philips EM-301 electron microscope equipped with a high resolution stage and operated at 80 kV with a 50 micron objective aperture. In certain circumstances (see text) the specimen multilayers were treated with saturated uranyl acetate (pH 5) and lead acetate [32] stains in the manner routinely applied to tissue sections for electron microscopy.

X-ray diffraction

For X-ray diffraction experiments, between 20 and 50 bilayers were deposited on wafers or thin glass plates and diffraction patterns were recorded as described in detail previously [27]. A rotating anode X-ray generator designed by Dr. William Longley of this laboratory [33] produced copper $K\alpha$ X-radiation and all diffraction patterns were recorded at ambient conditions ($\approx 22^\circ\text{C}$ and 50% relative humidity). Structure amplitudes $|F(h)| = c\sqrt{hI(h)}$ were obtained where c is a constant, h is the number of the diffraction order, and $I(h)$ is the integrated intensity of order h . Electron density profiles were calculated by using the formula

$$\rho(x) \propto \sum_h \phi(h) |F(h)| \cos \frac{2\pi xh}{d}$$

where d is the repeat period, and where x is the distance normal to the lamellar surface and $\phi(h)$ is the phase of order h . For centrosymmetric systems the phase factors $\phi(h)$ are either +1 or -1 for each diffraction order. The procedures used for determining the phase factors are given in the results section.

Results

Both electron microscopy and X-ray diffraction results indicate that highly oriented asymmetric bilayers can be constructed by use of the Langmuir-Blodgett dipping technique. Several different types of asymmetrical bilayers have been analyzed, including those with asymmetries in head group type,

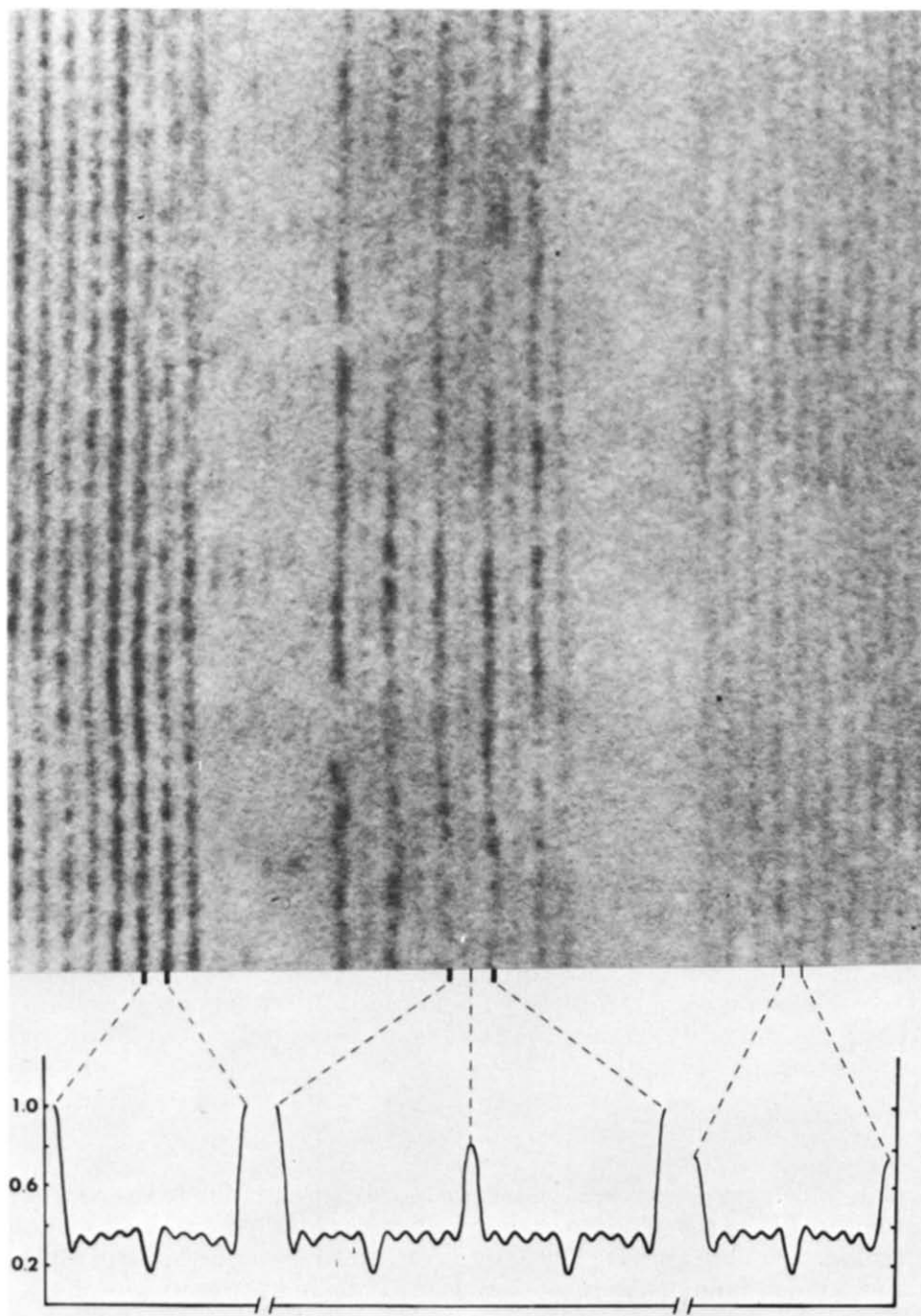


Fig. 2. Electron micrograph and corresponding electron density profiles of symmetric bilayers of barium behenate (left) and calcium behenate (right), and asymmetric bilayers of apposed barium behenate and calcium behenate monolayers (center). The lamellar contrast in these three zones of the micrograph is due to the barium carboxylate and calcium carboxylate head groups, and the zones are separated by bilayers of behenic acid, which give no lamellar contrast. The multilayers were unfixed, unembedded, and unstained. The vertical scale on the bilayer profiles gives their absolute electron densities in electrons/Å³. The distance between adjacent carboxylate head groups planes is measured to be 54 Å in the micrograph (top) and 58 Å in the X-ray diffraction derived profiles (bottom).

chain length distribution, and associated polypeptide distribution.

Model membranes with asymmetrical head group types were constructed as outlined in Methods by apposing monolayers of barium behenate and calcium behenate. These particular lipids were chosen as it has been shown in previous studies that the difference in electron density between the barium carboxylate and calcium carboxylate head groups can be detected by electron microscopy [26] and X-ray diffraction techniques [27]. Thus, these differences in head group densities can be used as an indicator for bilayer asymmetry. Moreover, the X-ray diffraction patterns from both barium behenate and calcium behenate bilayers have been rigorously interpreted by an isomorphous replacement technique [27]. Symmetric bilayers of barium stearate have also been analyzed by deconvolution methods [34].

Fig. 2 shows both an electron micrograph of an unstained multilayer and the corresponding bilayer electron density profiles derived from the X-ray analysis. The micrograph can be readily related to the native molecular structure of the multilayers since the specimen was not treated with stains, fixatives or embeddings. The lamellar zone appearing to the far left of the Fig. 2 micrograph corresponds to symmetric bilayers having apposed molecules of barium behenate, whereas the lamellar zone appearing on the far right corresponds to bilayers of calcium behenate. We have shown previously that the electron lucent lines of the lamellae represent the hydrocarbon interiors of the centrosymmetrically arranged bilayers and that the electron dense lines correspond to the headgroup regions of the bilayers [26]. Note that the dark lamellae in the barium behenate region (left) are considerably darker than the lamellae in the calcium behenate region (right). This is due to the greater mass density of the barium carboxylate headgroup [26]. Electron density profiles of both barium and calcium behenate have been calculated on an absolute electron density scale [27] and are shown immediately below the corresponding zones of the micrograph. Notice that the two profiles are nearly identical except for the much higher electron density in the head group regions of barium behenate (about $1.0 \text{ electron/\AA}^3$) than in the head group regions of calcium behenate (about $0.7 \text{ electron/\AA}^3$). Both profiles have broad, flat regions having an electron density of about $0.34 \text{ electron/\AA}^3$ between the headgroups. These low density areas correspond to the hydrocarbon chain regions of the bilayer. The sharp dip in the center of the profile has been attributed to the localization of the terminal methyl groups of the lipid molecules in the bilayer [34].

The differences in density of the barium and calcium carboxylate head groups have been used as indicators of bilayer chemical asymmetry. The central lamellar zone shown in the Fig. 2 micrograph was formed by apposing monolayers of barium and calcium behenate. In this zone there is an alteration of darker and lighter head group planes. This can best be seen by tilting the micrograph and viewing these asymmetric bilayers in a direction parallel to the lines. By reference to the multilayer deposition sequence it is known that the dense line on the left edge of the asymmetric zone arises from barium head groups whereas the lighter line on the right edge of this zone corresponds to calcium head groups. It can be seen that there are nine asymmetric barium behenate/calcium behenate bilayers in the center zone of the micrograph with the left most line being barium and the right most being calcium. The dark barium

carboxylate lines have approximately the same density as the lamellae of symmetric barium behenate in the far left zone, while the lighter calcium carboxylate lines have the same density as the lamellae of symmetric calcium behenate in the far right zone. This indicates that it has been possible to segregate calcium carboxylate and barium carboxylate head groups to the opposite sides of the same bilayer.

The X-ray diffraction results are in accord with this interpretation. Fig. 3A is a low-angle diffraction pattern from symmetric barium behenate bilayers, $d = 58$ Å, while Fig. 3B is a diffraction pattern of asymmetric barium behenate/calcium behenate bilayers, $d = 116$ Å. Note that the intensity distribution for the even orders of the pattern in Fig. 3B is almost exactly the same as the distribution of intensities in Fig. 3A. The major difference between the two patterns is the presence of weak odd order reflections in the $d = 116$ Å asymmetric barium behenate/calcium behenate pattern. Orders 3, 5, and 7 of the 116 Å repeat are marked with arrows in Fig. 3B. The first order is lost in the beam stop scatter in this exposure, but can be resolved with shorter exposure times and longer specimen-to-film distances. (Again it should be pointed out that although each bilayer in this specimen is asymmetric, there is a center of symmetry between adjacent bilayers and thus the unit cell of $d = 116$ Å contains two bilayers and is centrosymmetric. Therefore all diffraction orders of $d = 116$ Å have either a positive or negative phase factor). The fact that the even orders of the barium behenate/calcium behenate pattern have an almost identical intensity distribution to the reflections of the symmetric barium behenate pattern implies that these reflections have the same phase combination in both cases. The phases of the first nine orders of barium behenate have been determined previously [27] to be all positive. The phases of orders 1, 3, 5, and 7 from the barium behenate/calcium behenate pattern were determined by making the assumption that one half of the bilayer should have a profile similar to that of barium behenate. The combination of all orders, even and odd, with positive phases, satisfied this assumption most satisfactorily.

The resulting electron density profile shown in the center of Fig. 2 is on the same absolute electron density scale which was previously calculated for symmetric barium behenate bilayers [27]. Notice that this profile represents two asymmetric bilayers with the head group plane sequence being barium carboxylate, calcium carboxylate, and then barium carboxylate again. For this pair of asymmetric bilayers, the barium carboxylate head group has the same electron density as the symmetric barium behenate profiles (left) and the calcium carboxylate head group has the same electron density as the symmetric calcium behenate profile (right). It can be seen that both the symmetric and asymmetric bilayers have uniform low electron density hydrocarbon chain regions with sharp terminal methyl dips located in the geometric centers of each of the bilayers. Thus, both the electron microscopic and X-ray diffraction results show that highly oriented lipid bilayers with asymmetric divalent cation head group distributions can be formed by the joining together of separate monolayers.

Since many biological membranes are composed of lipids having different hydrocarbon chain lengths we have considered the effects of such chemical variations upon the ultrastructure of model systems. In this regard we were par-

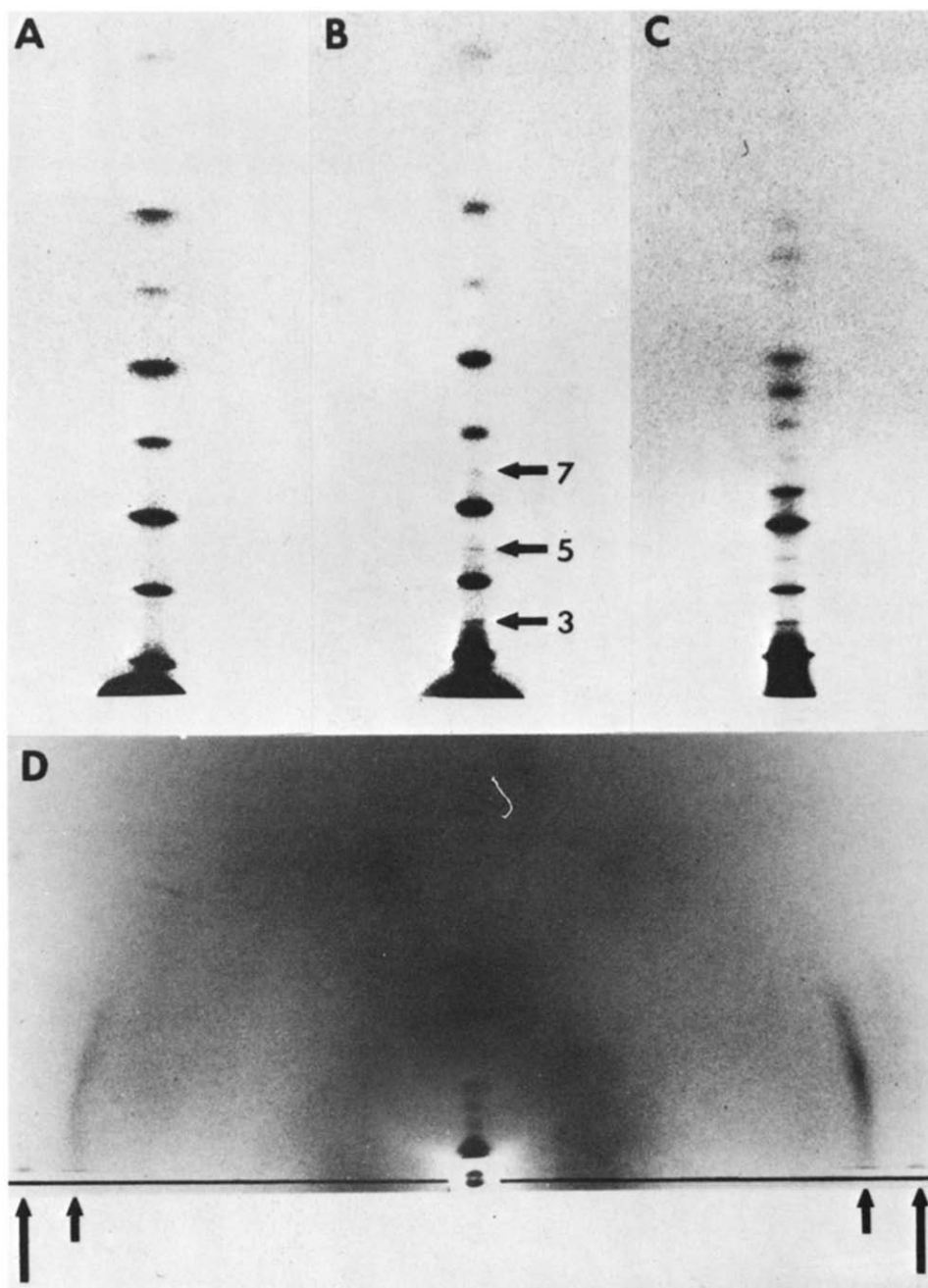


Fig. 3. X-ray diffraction patterns from (A) barium behenate bilayers, (B) asymmetric barium behenate/calcium behenate bilayers, (C) asymmetric barium behenate/behenic acid-polylysine bilayers, and (D) symmetric behenic acid-polylysine bilayers. In each case, one half of the diffraction pattern is shown. The patterns of A, B, and C were taken at the same specimen-to-film distance, while D was taken at a much shorter distance so the wide-angle reflections at 3.7 Å (long arrows) and 4.1 Å (short arrows) could be recorded. In D a narrow horizontal black line has been drawn in on the equator of the X-ray film. Before the exposure was taken, the beam stop was removed for a few seconds so that the direct beam is seen in the middle of the equator as a black circle. The light line through this circle is due to absorption by the specimen and glass support. Note that the 3.7 Å reflection is directly on the equator and is partially obscured by the shadow of the glass support. Due to the tilt of the hydrocarbon chains in the bilayer, the 4.1 Å reflection is located off the equator so that a line drawn from the center of this reflection to the image of the direct beam makes an angle of 17° relative to the equator. The meridional lamellar reflections have repeat periods of (A) 58 Å, (B) 116 Å, (C) 127 Å, and (D) 69 Å and extend to about $1/6 \text{ \AA}^{-1}$ in reciprocal space. The odd orders 3, 5, and 7 are indicated by arrows in pattern B.

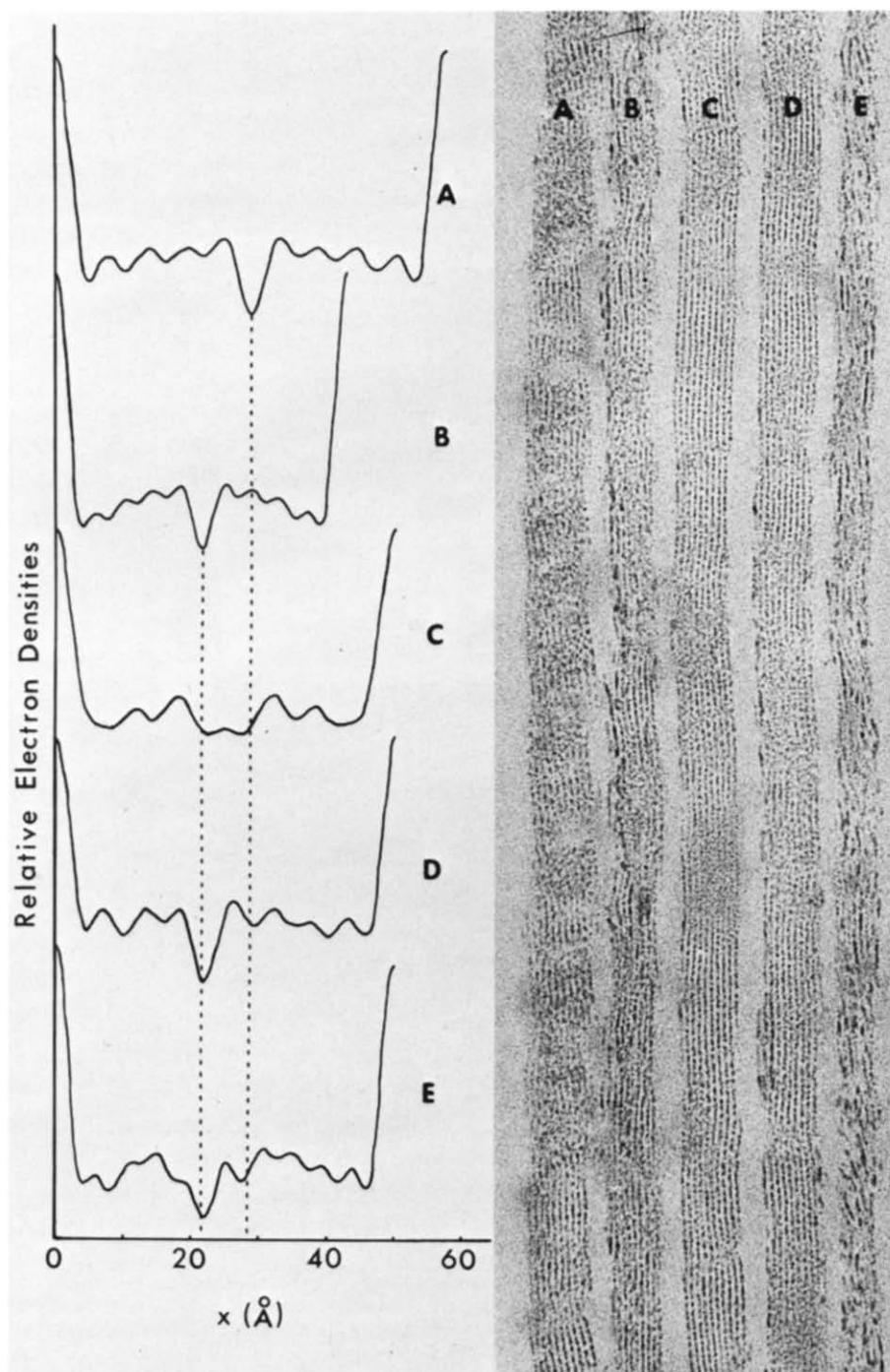


Fig. 4. Electron density profiles and electron micrograph of (A) barium behenate bilayers, (B) barium palmitate bilayers, (C) symmetric bilayers formed from apposed mixed monolayers of barium behenate and barium palmitate (1 : 1 molar ratio), (D) asymmetric bilayers with barium behenate and barium palmitate segregated to apposing monolayers, and (E) asymmetric bilayers with barium palmitate and behenic acid in apposing monolayers. In each case, the electron density profile of one bilayer is shown. For the symmetric cases of A, B, and C this corresponds to the entire unit cell, while for the asymmetric bilayers of D and E this corresponds to one half of the unit cell. Resolution of all profiles is between 6 and 7 Å. In the micrograph, the lamellar zones A, B, C, D, and E are separated by clear zones of behenic acid bilayers and in zone A the distance between barium carboxylate head group plane is 54 Å.

ticularly interested in determining the consequences of having molecules of different lengths mixed in each monolayer of the bilayer and in having chains of dissimilar lengths segregated to opposite sides of the bilayer. Both the microscopic and X-ray diffraction results of these studies are summarized in Fig. 4.

In the first case control multilayers of barium behenate (22 carbon atoms), similar to those shown in zone A of the Fig. 4 micrograph, were analyzed by diffraction methods and were found to have an X-ray repeat period of 58 Å. Wide angle patterns from barium behenate bilayers have been published previously [27] and show that the unit cell is monoclinic with the hydrocarbon chains having a tilt of 18° relative to the normal to the plane of the bilayer. Multilayers of barium palmitate (16 carbon atoms), similar to those seen in zone B of the Fig. 4 micrograph, were analyzed by X-ray diffraction and were found to have a repeat period of 43 Å. In this case, the wide-angle pattern consisted of single spots located directly on the equator at a spacing of 4.1 Å. This implies that the unit cell is hexagonal and the chains are oriented perpendicular to the plane of the bilayer. The difference in the wide-angle patterns from barium behenate and barium palmitate can be explained by the monolayer properties of the two compounds. It has been shown [35] that fatty acids with over 20 carbons in their chains, such as behenic acid, form two high pressure condensed phases, the S phase in which the chains are in an hexagonal configuration and the CS phase in which the chains are in a monoclinic configuration. Fatty acids with fewer than 20 carbons have only one phase, the hexagonal S phase. Thus prior to transfer, the barium behenate monolayer was in the CS phase and the barium palmitate monolayer was in the S phase. The repeat periods are in excellent agreement with the expected chemical width of bilayers of these compounds when consideration is given to the number of carbon atoms, the bond angles and the hydrocarbon chain tilt. Electron density profiles of the barium behenate shown in Fig. 4A and barium palmitate shown in Fig. 4B indicate that both types of bilayers have similar symmetric structures with high density head groups adjacent to lower density hydrocarbon chain regions with very low density terminal methyl troughs in the geometric centers of the bilayers.

We next designed an experiment to evaluate the ultrastructural effect of having molecules of dissimilar chain lengths mixed together in the same monolayer. Symmetric bilayers were formed from a single monolayer having an equimolar mixture of barium behenate and barium palmitate. The X-ray diffraction pattern obtained from these mixed bilayers consists of eight sharp orders of a single repeat period, 50 Å. This periodicity is approximately the average of the periods of barium behenate and barium palmitate bilayers. The intensity distribution of the mixed bilayer pattern is very similar to those of both barium behenate and barium palmitate with slight differences in intensity distribution in orders 6–8. It was therefore assumed that the first five orders of diffraction had the same phase combination as the pattern from pure barium behenate bilayers. The criterion used for choosing the phase combination for orders six, seven, and eight was that the hydrocarbon chain region of the bilayers should be relatively flat except near the terminal methyl regions. The favoured phase choice gave the Fourier synthesis shown in Fig. 4C. This electron density profile of the mixed chain bilayer contains a low density dip in the

center of the bilayer, but this trough has broadened considerably. However, the head group region of the mixed bilayer is still a sharp peak. This, together with the lamellar orderlines of the micrograph in this region (Fig. 4C) indicates that the effect of mixing fatty acid chains in the same bilayer is to delocalize the terminal methyl ends of the hydrocarbon chains, while leaving the polar head groups in register. An important point to note is that the wide-angle pattern from the mixed bilayer is exactly the same as the pattern from pure barium palmitate bilayers. In each case there is a sharp equatorial reflection at a spacing of 4.1 Å.

Oriented lipid bilayers with an asymmetric fatty acid chain length distribution were constructed by transferring barium behenate and barium palmitate to a glass or epoxy support on alternate dipping cycles. The X-ray diffraction pattern from the array of asymmetric bilayers consists of 18 sharp diffraction orders of a periodicity of 101 Å. Again the odd orders of diffraction are relatively weak. Phases for each diffraction order were assigned assuming that one side of the bilayer should have a profile similar to that of symmetric barium behenate and the other side should look like symmetric barium palmitate. It should be noted that the phases of all but the weakest order could be determined unambiguously by this method, since alternative phase choices produce obvious anomalies in the profile such as large positive peaks in the middle of the hydrocarbon chain region. The resulting profile and electron micrograph of the asymmetric barium behenate/barium palmitate bilayer are shown in Fig. 4D. Note that in the profile the terminal methyl dip is very sharp, but is not in the geometric center of the bilayer. Thus, the terminal methyl groups of all lipids are localized at a position away from the center of the bilayer. The trough has been shifted away from the center of the bilayer by an amount equal to the difference in chain lengths of barium behenate and barium palmitate monolayers ($29 \text{ Å} - 22 \text{ Å} = 7 \text{ Å}$). Note that the bilayers in Fig. 4C and D are chemically identical (i.e. 1 : 1 molecular ratio) but that they are physically different. In the profile of Fig. 4C the different chain lengths have been mixed together on both sides of the bilayer, while in Figs. 4D the different chain length molecules have been segregated into apposing monolayers. While the structural differences between them is evident in the X-ray results, these two kinds of bilayers can not be distinguished by electron microscopy. That is, the diffraction patterns and resulting electron density distributions of Figs. 4C and D are quite different, but regions Figs. 4C and D are indistinguishable in the micrograph.

Thus, the Langmuir-Blodgett method can be used to produce bilayers with either asymmetric divalent cation head groups or asymmetric hydrocarbon chain distributions. In both cases, the asymmetry seems to be maintained and there is no indication of spontaneous transposition between monolayers.

However, this is not always the case. We have reported earlier [26,27] that barium behenate and behenic acid molecules can spontaneously invert across asymmetric bilayers. In order to clarify the molecular nature of this self-mixing process we have designed experiments in which lipids of both different chain lengths and head group composition were used to identify opposite sides of the bilayer. Asymmetric bilayers were assembled by apposing monolayers of barium palmitate and behenic acid. Consideration of the Langmuir-Blodgett

dipping process (Fig. 1) of forming bilayers from monolayers and noting that saponified carboxylate groups are microscopically visible while unsaponified carboxyl groups are not [26] leads to the expectation that 10 barium palmitate/behenic acid bilayers would produce a micrograph having 5 parallel dense lines spaced about 100 Å apart. The experimental result shown in zone E of Fig. 4 micrograph clearly demonstrates that the actual structure is quite different than that predicted. Considerable spontaneous mixing is evident with the approximately 10 dense lines having an image spacing of about 50 Å. That is to say that the electron dense barium appears on both sides of the "asymmetric" barium palmitate/behenic acid bilayers.

X-ray diffraction patterns from the barium palmitate/behenic acid multilayers contain 18 reflections with $d = 100$ Å. The reflections in these patterns are broadened compared to the reflections in patterns from the specimens described in Figs. 4A, B, C, and D. An electron density profile of these bilayers was calculated by assuming that the interior of the bilayers should be of low density and flat except for the terminal methyl trough region. The resulting profile shown in Fig. 4E has similarities to the previous cases in which bilayers were asymmetric in either the head group or hydrocarbon region but it can be seen that mixing has occurred across the bilayer. We have previously shown that the absolute electron density of barium carboxylate is approximately two times that of the unsaponified carboxyl group [27] yet the profile shown in Fig. 4E indicates that the barium/carboxyl "asymmetric" bilayer has nearly equal head group density on both sides. Moreover, while the terminal methyl dip is situated to one side of the geometric center of the bilayer as was the case for asymmetric chains (Fig. 4D) it is also broadened as was the case for bilayers having intentionally mixed chain lengths (Fig. 4C). Thus, both the head group and hydrocarbon asymmetry indicators have become mixed suggesting that the entire lipid molecule participates in the bilayer "flip-flop". This result is in agreement with our earlier conclusion [26] that the transposition is an ensemble inversion similar to X-Y redistributions of the Langmuir-Blodgett type [29,36,37].

Thus, the available evidence indicates that spontaneous translational migration does not occur in asymmetric bilayers having dissimilar carboxylate head groups (Fig. 2) or dissimilar hydrocarbon chain lengths (Fig. 4D) but that carboxylate/carboxyl head group asymmetry induces molecular translation across the bilayer (Fig. 4E).

It has been shown by others that synthetic polypeptides such as poly-L-lysine will associate with fatty acid monolayers and will change the electrical properties of planar bimolecular lipid bilayers [38]. Therefore, lipid-peptide monolayers of this type were incorporated into multilayers in planned assemblies of both symmetric and asymmetric bilayers. In accordance with the careful design of the electron microscopic aspects of this and previous studies [26], the lipid-peptide multilayers were first examined in their untreated state. It was found that bilayers associated with polylysine produced no lamellar image and that zones of the specimen which were composed of lipid-peptide bilayers were indistinguishable from zones of pure behenic acid. This can be seen in the micrograph on the left hand side of Fig. 5 which contains regions of (A) barium behenate bilayers, (B) behenic acid bilayers, (C) asymmetric bilayers with

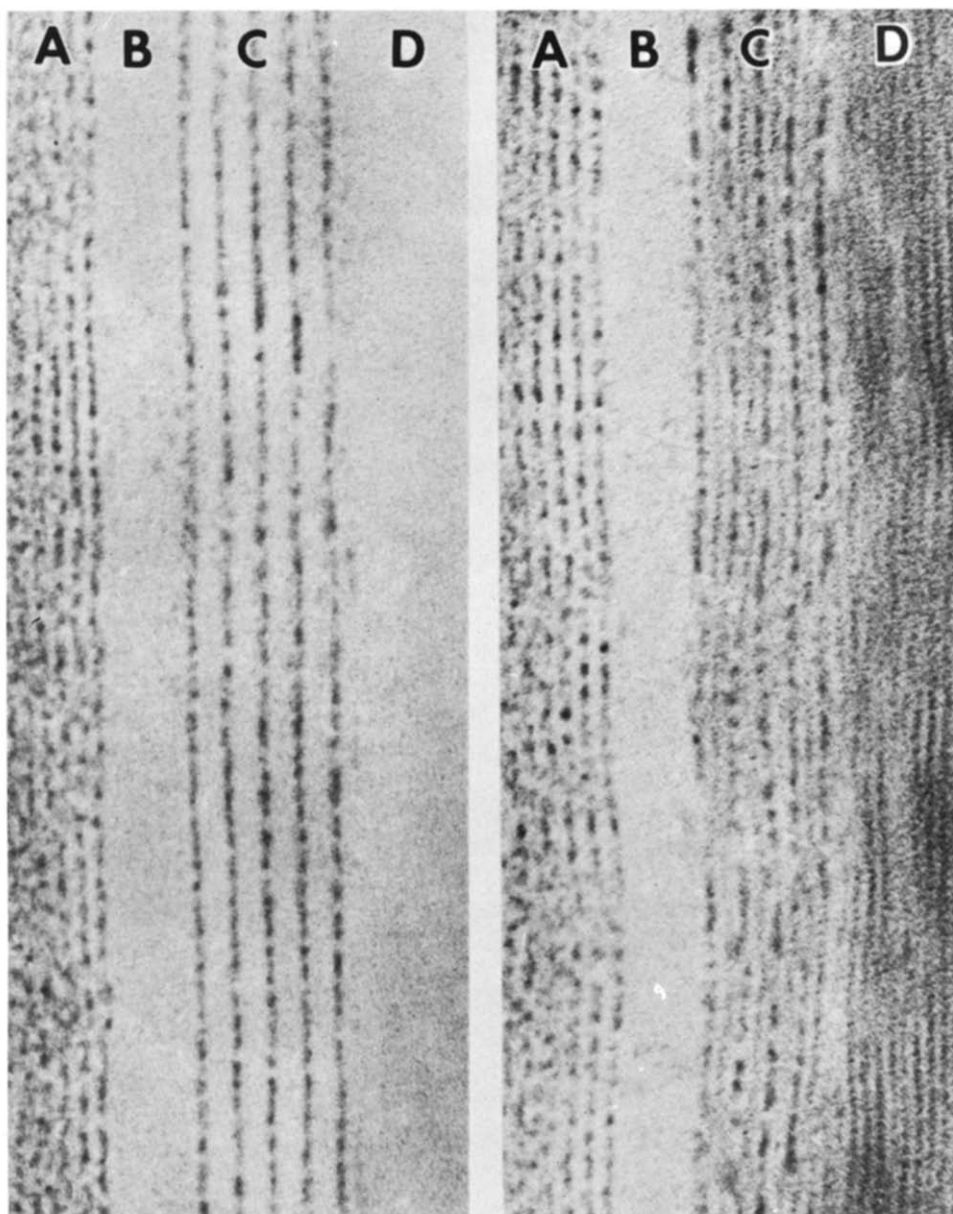


Fig. 5. Electron micrographs containing zones of (A) barium behenate bilayers, (B) behenic acid bilayers, (C) asymmetric bilayers with barium behenate and a behenic acid-polylysine complex in apposing monolayers, and (D) symmetric bilayers of the behenic acid-polylysine complex. The multilayers in the micrograph on the left were unstained, while those on the right were section stained with uranyl acetate for 15 min. Regions A and B are unaffected by the staining procedure, while the polylysine regions of the multilayers are stained in C and D. In region A the distance between barium carboxylate head group planes is 54 Å.

barium behenate and a behenic acid-polylysine complex in apposing monolayers, and (D) symmetric bilayers of the behenic acid-polylysine complex. Consequently, efforts were made to enhance selectively the electron contrast of

the peptide component of the multilayer by staining freshly cut sections with uranyl acetate. The micrograph on the right hand side of Fig. 5 shows that this section staining procedure results in the development of considerable lamellar density in those zones of the multilayer with polylysine containing bilayers. Although the staining introduces some disorderliness into the multilayer, careful measurement of the lamellar spacing of zone D shows it to be of bilayer dimensions (approx. 50 Å). It can also be seen that after the staining procedure dark lamellae appear alternating with the barium carboxylate lines in region C. These stained lamellae are the behenic acid-polylysine complexes in the asymmetric barium behenate/behenic acid-polylysine bilayers. It should be emphasized that the number of both the barium carboxylate and stained polylysine lamellae correspond to the number expected from the transfer model of Fig. 1. The completeness of the molecular segregation in these asymmetric lipid-peptide bilayers can be best appreciated by closely examining this zone C of the specimens.

In the pairs of micrographs Fig. 6A and B and Figs. 6C and D high magnification images of the stained and unstained asymmetric bilayers have been aligned with respect to the barium behenate lines. By tilting Fig. 6 to a low angle and looking parallel to the lamellae it can be seen that the barium head groups appear as a row of dots whereas the uranyl acetate plus lead stain lines (Fig. 6B) appear uniformly dense. Comparison of the unstained (Fig. 6C) bilayers with those exposed only to uranyl acetate (Fig. 6D) reveals that these stain lines have a granular texture. The segregation of the heavy metal stain reaction to one side of asymmetric units indicates that molecular inversions do not occur in asymmetric barium behenate/behenic acid-polylysine bilayers. This conclusion is supported by the orderliness of the asymmetric barium head group planes of both the unstained and stained specimens.

Specimens consisting of a number of asymmetric barium behenate/behenic acid-polylysine bilayers were also made for X-ray diffraction analysis. The resulting low-angle diffraction pattern is shown in Fig. 3C. Note the sharpness of the reflections. There are 18 lamellar orders of a periodicity of 127 Å. The phases for these orders were determined assuming that one side of the bilayer should look like a monolayer of barium behenate. From consideration of the transfer model (Fig. 1) and the micrographs of Figs. 5 and 6 this appears to be a valid assumption. The resulting electron density distribution for two asymmetric bilayers is shown in Fig. 7. The left hand side of the first bilayer from $x = 0$ to $x = 29$ Å is a monolayer of barium behenate while the right hand side from $x = 29$ Å to $x = 63$ Å is a behenic acid-polylysine complex. Since an absolute electron density scale has previously been derived for barium behenate [27] and is included on the ordinate of the plot in Fig. 7, the behenic acid-polylysine complex is also on an absolute scale. The behenic acid-polylysine side of the bilayer is about 5 Å wider than the barium behenate side. There is an extra layer of electron density of 0.6 electron/Å³ on the outer edge of this side of the bilayer which is undoubtedly polylysine.

In order to obtain more information on the structure of the behenic acid-polylysine complex, X-ray diffraction experiments were performed on symmetric bilayers. The low angle pattern contains 9 orders of a 69 Å periodicity. The phases of these orders were assigned assuming the profile should be consis-

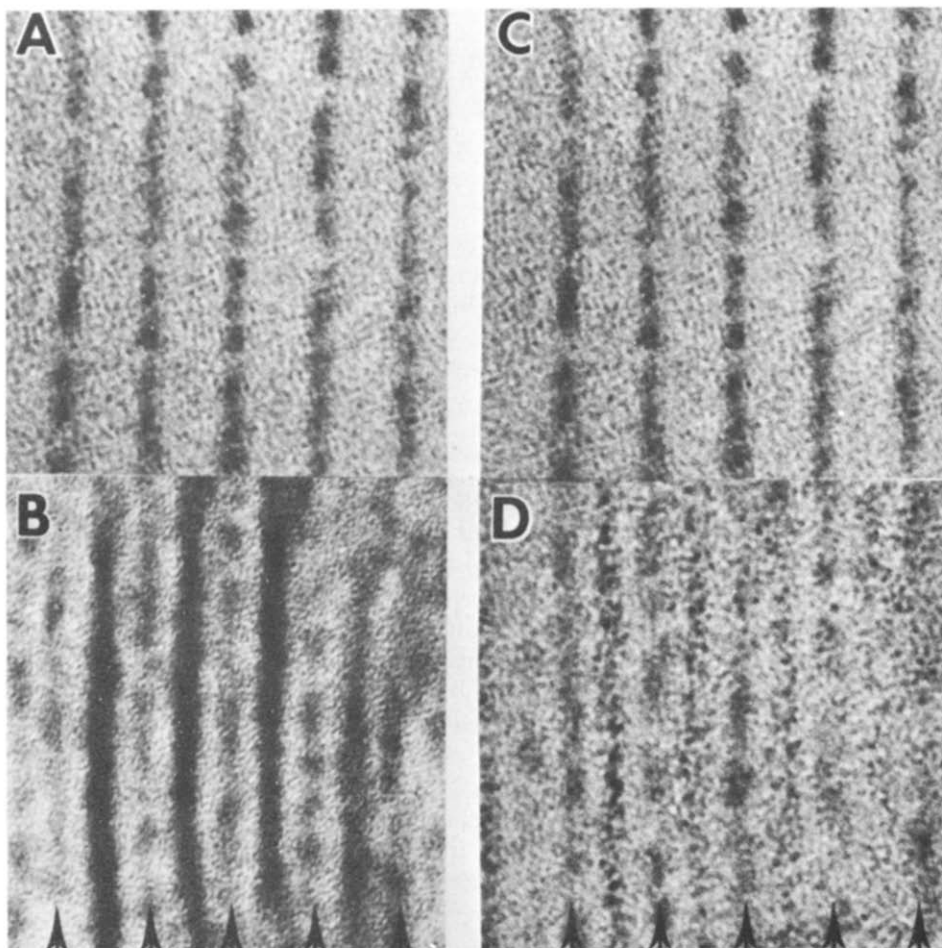


Fig. 6. High magnification micrographs of eight asymmetric bilayers having apposed monolayers of barium behenate and a behenic acid-polylysine complex. Bilayers in A and C were unstained and only the barium carboxylate head groups can be seen. The distance between the barium carboxylate head group planes is approx. 110 Å. In B the sections were stained with uranyl acetate and lead and in D the sections were stained with uranyl acetate only. In both B and D the stained polylysine is visible and can be distinguished from the barium carboxylate head groups in the apposing monolayer. The arrow heads at the bottom of the figure point along the barium carboxylate head groups of both stained and unstained bilayers. The location of the polylysine in B and D can best be seen by tilting the page and viewing the figure in the direction of the arrows.

tent in appearance with the monolayer from $x = 29$ Å to $x = 63$ Å in Fig. 7. All nine orders could be phased unambiguously by making this assumption and the electron density profile is shown in Fig. 8A. Note that the central 49 Å (from about $x = 10$ Å to $x = 59$ Å) of the bilayer looks like the central region of a barium behenate or behenic acid bilayer (see Fig. 4A and Fig. 9 of ref. 27). To interpret the profile of Fig. 8A on a molecular level, it is important to know the chain packing and chain tilt parameters which can be determined from the wide-angle diffraction pattern shown in Fig. 3D. In a previous study [27], it was shown that pure behenic acid bilayer chains are packed in a monoclinic

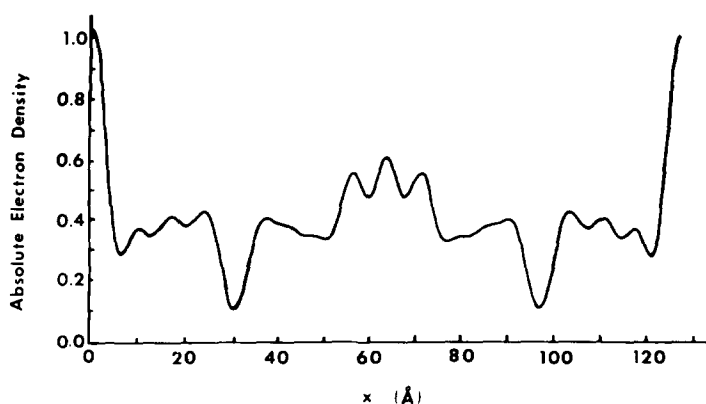


Fig. 7. Electron density profile of two asymmetric bilayers each of which contains barium behenate in one monolayer and a behenic acid-polylysine complex in the apposing monolayer. The barium carboxylate head groups are centered at $x = 0$ Å and $x = 127$ Å, while the polylysine is centered at $x = 63.5$ Å. The vertical scale gives the absolute electron density in electrons/Å³.

subcell and have a chain tilt of 27° relative to the normal to the plane of the bilayer. The wide-angle pattern from the lamellar behenic acid-polylysine complex (Fig. 3D) is similar to the wide angle pattern from pure behenic acid bilayers (see Fig. 2B, ref. 27) in that both patterns contain reflections at 3.7 Å and 4.1 Å. However, the orientation of the 4.1 Å reflection on the X-ray film is different in the two cases, indicating that the presence of polylysine alters the

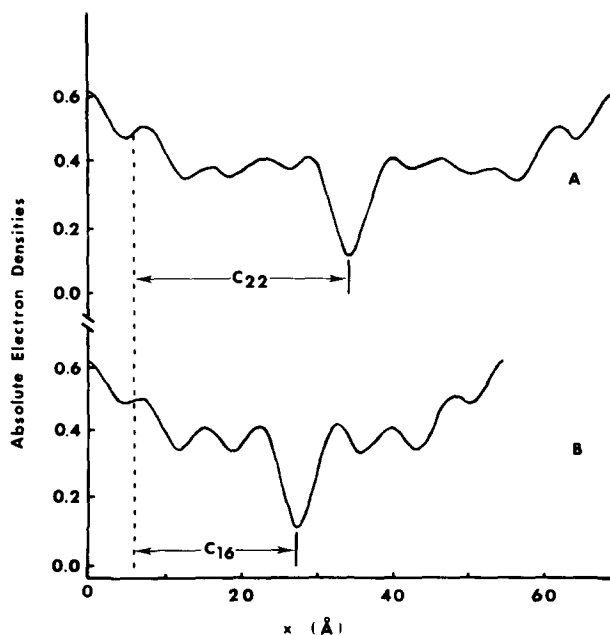


Fig. 8. Absolute electron density profiles of symmetric bilayers of (A) behenic acid-polylysine and (B) palmitic acid-polylysine. The dotted line denotes the furthest extent of the fatty acid from the center of the bilayer.

lipid chain tilt. In Fig. 3D the outer reflection, marked by long arrows, is a spot at a spacing of 3.7 Å which is located directly on the equator and is partially obscured by the shadow of the glass specimen support. The second reflection, marked by short arrows, is an arced spot at a spacing of 4.1 Å which is centered at an angle of about 17° relative to the equator, or 107° relative to the meridional low-angle spacings. By analogy to the case of behenic acid [27], it can be assumed that the unit cell of the behenic acid-polylysine complex is monoclinic, with the observed diffraction spots being the (020) and (110) reflections, with the (110) reflection making an angle of approximately 107° relative to the meridional reflections. For the Langmuir-Blodgett type multilayers, the planes of the bilayer are equivalent to the (001) reflecting planes. Thus, the angle between the (001) and (110) reflecting planes is known, and it is a straightforward matter to calculate the angle between the (001) and (200) reflecting planes from the formula in ref. 39. The calculations show that the chains are tilted 110° relative to the shortest axis (the *a* axis) of the unit cell. In other words, the hydrocarbon chains are tilted 110° relative to the plane of the bilayer or tilted 20° relative to the normal to the plane of the bilayer. It can be estimated from crystallographic data [40] that if a bilayer were formed from two fully extended behenic acid molecules oriented perpendicular to the plane of the bilayer it would have a width of about 61 Å. Therefore, considering the 20° chain tilt, the contribution of the fatty acid molecules to the width of the behenic acid-polylysine complex is approximately 57 Å (since $61 \text{ Å} \cos 20^\circ = 57 \text{ Å}$). Thus, the lipid portion of the behenic acid-polylysine complex extends from about $x = 6 \text{ Å}$ to $x = 63 \text{ Å}$ on the profile of Fig. 8A. The high density peaks centered at $x = 0 \text{ Å}$ and $x = 69 \text{ Å}$ must be caused entirely by the polypeptide as they are too far from the terminal methyl dip to be caused by behenic acid. The peaks centered at $x = 7 \text{ Å}$ and $x = 62 \text{ Å}$ are primarily caused by the carboxyl groups of the lipid. The centers of these peaks are within about 1 Å of the edges of the lipid bilayer (denoted by a dotted line in Fig. 8) and have an electron density of just slightly greater than 0.5 electron/Å³. In previous studies [27], we have determined the absolute electron density of the carboxyl groups in pure fatty acid bilayers to be 0.5 electron/Å³. The slight difference in these two values and the fact that the peaks at $x = 7 \text{ Å}$ and $x = 62 \text{ Å}$ in Fig. 8A are slightly wider than the head group peak in pure fatty acid bilayers (see Fig. 9 of ref. 27) might be caused by some penetration of polylysine into the head group region of the bilayer. However, the polylysine does not penetrate into the hydrocarbon chain region of the bilayer as the absolute electron density of the hydrocarbon chain regions are the same for the behenic acid-polylysine complex and for pure behenic acid or barium behenate bilayers. This can be seen quite clearly in the profile of the asymmetric barium behenate/behenic acid-polylysine complex (Fig. 7) where the absolute electron density is the same for the hydrocarbon chains on both sides of the asymmetric bilayers. Moreover, the central region of the bilayer, from about $x = 12 \text{ Å}$ to $x = 57 \text{ Å}$ looks identical to pure behenic acid (see Fig. 9 of ref. 27). The width of the polylysine layer between the bilayers is difficult to determine precisely, but from the profile of Fig. 8A, the polylysine must extend from $x = 0 \text{ Å}$ to at least $x = 8 \text{ Å}$ and possibly to $x = 11 \text{ Å}$. This means that the polylysine penetrates between 2 and 5 Å into the fatty acid bilayer, or, in other words, just

into the head group region. An experiment was performed to verify this molecular interpretation and to aid in distinguishing between lipid and polypeptide in the electron density profile. X-ray diffraction patterns were recorded from lamellar palmitic acid-polylysine complexes and the resulting electron density profile is shown in Fig. 8B. The shape of this curve is very similar to that of Fig. 8A, as both contain relatively high density polylysine regions on the outside of the profiles and flat hydrocarbon chain regions with sharp terminal methyl troughs in the center of the profiles. The major difference in the two profiles is in the width of the profiles. The theoretical length of the fatty acid molecules measured from the center of the bilayer is indicated by arrows in both Figs. 8A and B. In both profiles the lipid extends to the same position with respect to the polylysine region, as indicated by the vertical dotted line. Thus, the width of the polylysine layer is the same when associated with bilayers having different hydrocarbon chain lengths. The similarity in shape of the two curves also indicates that the polylysine penetrates into the lipid bilayer by the same amount (between 2 and 5 Å) in both cases.

The conformation of the polylysine in the lipid-peptide bilayers is unknown since no X-ray reflections were recorded which could be attributed solely to the polylysine molecule. It was also impossible to obtain X-ray diffraction data on the stained lipid-peptide multilayers since, although these sections could be stained for electron microscopy, the entire specimen could not be "block stained" as the stain did not penetrate the multilayers.

It should be noted that the repeat periods in the X-ray diffraction patterns are always somewhat larger than those measured in the electron micrographs for both fatty acid salts and fatty acid-polypeptide complexes. The shrinkage in the electron image might be attributed to dehydration effects due to the high vacuum of the microscope in the case of fatty acid-polypeptide multilayers, but dehydration can not be a factor for the barium behenate bilayers, as it has been shown [41] that multilayers of this compound contain no water. It is likely that the reduced spacing is primarily due to disruption of the bilayer hydrocarbon region by the electron beam [26] as electron beam irradiation of untreated lipid is known to cause a disordering of the hydrocarbon structure through a process of ionization and chain cross linking [42,43]. Thus, the electron beam may tend to "fix" the hydrocarbon region of the bilayer. However, the beam damage effects are self limiting in that a constant bilayer thickness is rapidly attained after electron illumination. We are currently attempting low dose electron imaging to determine exactly how much of the shrinkage can be attributed to electron beam damage.

Discussion

While it is known that biological membranes are asymmetrical structures consisting primarily of lipids and proteins, many details of their molecular organization are unknown. We have studied model membrane systems having well defined geometry and chemical composition in order to obtain information on the manner in which lipids and lipid-peptide complexes self organize. We have previously shown that the natural electron imaging properties and the electron density distribution of fatty acid bilayers can be unequivocally linked

to the molecular substructure of the bilayer [26,27]. In the present study we have used the intrinsic structural characteristics of lipid and peptide molecules to identify their location in asymmetric bilayers. It has been found that molecular features such as head group density, terminal methyl density, chain length, chain tilt, and stain reactivity can be used to determine the distribution of molecules across the bilayer. Moreover, we have taken advantage of the geometry of the asymmetric bilayer to interpret the X-ray diffraction data.

The construction of bilayers having well defined chemical asymmetry depends on the reliability of the monolayer transfer process. An essential requirement of this approach is that molecules of apposed monolayers do not mix during the formation process. By reference to the Langmuir-Blodgett transfer operation [26] it can be expected that the alternate cycling of the solid support through different monolayers would result in a multilayer of the type shown in Fig. 1. The validity of this transfer model was first tested by apposing monolayers of barium behenate and calcium behenate. The micrograph and the absolute electron density profiles (Fig. 2) indicate that little mixing occurs between the two kinds of saponified monolayers. Also, mixing was not evident when saponified fatty acids of different chain lengths were segregated to opposite sides of the bilayer, as evidenced by the position and sharpness of the low density trough in the profile of asymmetric barium palmitate/barium behenate bilayers (Fig. 4D). The distance between the trough and the geometric center of the bilayer corresponds to the difference in thickness of the two apposed monolayers (see Figs. 4A and B).

When the barium behenate and barium palmitate molecules were intentionally mixed in both monolayers it was observed that the terminal methyl dip was located at the geometric center of the bilayer but was considerably broadened (Fig. 4C). The increase in width of this broadened trough corresponds to the difference in chain lengths between barium behenate and barium palmitate, as has been indicated by the dotted lines on the profiles in Fig. 4. The head group planes of both sides of the bilayer are well oriented and parallel with no indication of local steps or waves of the type which have been observed in phospholipid/water systems [44]. Since the head groups are in register, there are a limited number of possible ways, shown in schematic form in Fig. 9, in which the behenate and palmitate molecules can be arranged in the mixed bilayer. The arrangement shown in Fig. 9A in which like molecules are apposed can be excluded because the bilayer thickness would be larger than the experimentally observed repeat period. The overlapped molecular structure of Fig. 9B is unreasonable since the increased chain separation is inconsistent with the monolayer area/molecule measurements, the wide-angle X-ray spacing, and the head group densities observed in the electron micrographs. The bent chain configuration of Fig. 9C is also unsatisfactory because the angular distribution in the orientation of the chains would produce arcing in the wideangle reflections, and no arcing was observed. The arrangement of Fig. 9C is also unlikely because of the spacing requirements of the bent chains. The arrangement of apposing pairs of behenate and palmitate molecules shown in Fig. 9D is preferred as it is consistent with all experimental data, including bilayer thickness, interchain spacing, terminal methyl delocalization, and head group density. It should be noted that in the configuration of Fig. 9D the terminal methyl groups

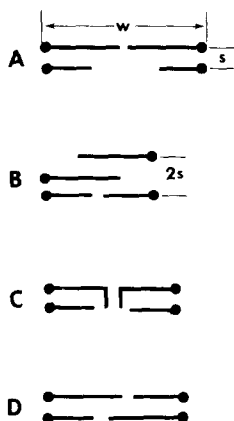


Fig. 9. Schematic diagram showing the possible molecular configuration for the symmetric bilayer of Fig. 4C which contains a one-to-one molar mixture of barium behenate (long chains) and barium palmitate (short chains). In A like molecules are apposed, in B there is an interpenetration of apposing long chain molecules, in C the long chains are bent, and in D there is a pairing of apposing long and short molecules. As described in the text, the experimental data favors model D. The letter "w" indicates the width of the bilayer while the letter "s" indicates the separation between adjacent hydrocarbon chains.

of each apposed behenate-palmitate pair are asymmetrically positioned in the bilayer. However, the terminal methyl regions are delocalized because behenate and palmitate molecules occur in equal numbers in both monolayers. This arrangement of molecules is very similar to that determined by Degerman and von Sydow [45] for the binary system of stearic acid and palmitic acid. However, the model of Fig. 9D is different than that proposed by Podo and Blasie [46] for mixed chain length phosphatidylcholine bilayers. The 13 Å resolution electron density profiles of Podo and Blasie [46] suggest that incorporation of shorter chain phosphatidylcholines into distearoyl phosphatidylcholine bilayers produces a reduction in the width of the hydrocarbon core of the mixed bilayer without a broadening of the terminal methyl trough. Their result is interpreted as being caused by "an increase of the gauche isomeric states around the carbon-carbon bonds within the longer chains" [46]. Thus, it appears that mixed fatty acid bilayers have a different hydrocarbon core structure than bilayers of mixed phosphatidylcholine chain lengths. The reason for this difference is unknown.

The hydrocarbon chain arrangement of Fig. 9D implies a self-organization process during mixed bilayer formation in which long and short molecules of the apposed monolayers become paired. Another spontaneous process which has been observed in some types of Langmuir-Blodgett multilayers is the translational diffusion of molecules across the bilayer [29,30,36,37,47]. When a fatty acid, behenic acid, was apposed to a fatty acid salt, barium palmitate, there was considerable rearrangement and disordering of the molecules in the bilayer as evidenced by the broadened X-ray diffraction reflections and the somewhat chaotic appearance of this region of the electron micrograph (Fig. 4E). The profile of Fig. 4E shows that not only is the head group density higher on the behenic acid side of the bilayer than would be expected from the transfer model of Fig. 1, but that the central region of the bilayer has a broadened terminal methyl trough, much like that of the intentionally mixed

chains (Fig. 4C). This shows that the entire barium palmitate molecule is involved in the "flip-flop". It has been suggested by others [37,48,49] that inversions in multilayers arise from the overturning of single monolayers. Since the overturning of single molecules could result in head-to-tail lipid arrangements, head group densities would appear at monolayer rather than bilayer spacings. No such peaks were found by either electron microscopic or X-ray diffraction analysis of the multilayers. It is more likely that pairs of apposed molecules exchange places across the bilayer in some cooperative manner during the formation process [29]. This is in accord with our earlier observation [26] that clusters of molecules exchange as bilayer ensembles.

Deamer and Branton [30] have studied the kinetics of this exchange by using ^{14}C -labelled stearate multilayers. They found that the exchange between monolayers occurred under water with a half life of 50 min in the presence of calcium in the subsolution and with a half life of 25 min in the absence of calcium [30]. These half lives are long compared to the time (a few seconds) the substrate stays under the water during each cycle of the Langmuir-Blodgett dipping procedure. Thus, the fact that we observe no flip-flop in either asymmetric barium behenate/calcium behenate bilayers (Fig. 2) or asymmetric barium palmitate/barium behenate bilayers (Fig. 4D) is consistent with the measurements of Deamer and Branton [30]. Apparently, however, the asymmetric fatty acid/fatty acid salt bilayers are considerably less stable with much shorter exchange half lives. It should be noted, however, that since the X-ray diffraction pattern does contain several odd orders of $d = 100 \text{ \AA}$ periodicity, some asymmetry is maintained and there is not a complete redistribution of molecules across the bilayer. While the mechanism of this "flip-flop" phenomenon is not fully understood, the crucial factor seems to be the difference in head group type. Thus, caution must be taken in interpretation of data from asymmetric bilayers formed from monolayers, either by the Langmuir-Blodgett [28,29] or Montal-Mueller [18] techniques. In both methods lipid monolayers are joined together.

When it can be shown that there is no molecular flip-flop, the formation of asymmetric bilayers can be a useful tool for X-ray diffraction analysis. In the case of the asymmetric barium behenate/behenic acid-polylysine multilayers, the unstained sections (Figs. 6A and C) indicate that barium behenate molecules stay segregated to one side of the bilayer, while the stained sections (Figs. 6B and D) show that the polylysine remains in the opposite side of the bilayer. So, although asymmetric barium behenate/behenic acid bilayers are quite unstable (see Fig. 3 of ref. 26), the asymmetric barium behenate/behenic acid-polylysine bilayers (Fig. 6) are stable and show no molecular flip-flop. Thus, polylysine stabilizes the bilayer.

The X-ray diffraction pattern of the asymmetric barium behenate/behenic acid-polylysine complex contains quite sharp lamellar reflections (Fig. 3C). The fact that the repeat period of $d = 127 \text{ \AA}$ is simply the sum of the repeat periods of barium behenate, $d = 58 \text{ \AA}$, and behenic acid-polylysine, $d = 69 \text{ \AA}$, is consistent with the transfer model of Fig. 1. The phase factor for each reflection was chosen assuming that one side of the bilayer should have a profile like that of barium behenate. This method of phase determination appears to be quite accurate, as a wrong phase choice produces an anomaly such as large peaks in

the hydrocarbon region of the barium behenate side of the bilayer. In general, the only reflections which can not be phased by this method are those so weak in intensity that they have little effect on the profile of the known side. Fortunately, however, such weak reflections also have little effect on the profile of the unknown side. Another advantage of this procedure is that if an absolute electron density scale has been determined for the reference side of the asymmetric bilayer, then the profile of the apposing side is also on an absolute electron density scale (Fig. 7).

The profiles of the lipid-peptide complexes (Figs. 8A and B) can be interpreted on a molecular level since the chain tilts and absolute electron densities can be compared to those of the pure lipid bilayers [27]. The polylysine residues can be compared to those of the pure lipid bilayers [27]. The polylysine resides on the outside of the bilayer, with only a slight penetration into the head group plane of the lipid bilayer. It is interesting to note that although the polylysine does not penetrate into the hydrocarbon chain region of the bilayer, it does change the chain tilt of the behenic acid molecules from 27 to 20°. We have also observed a change in tilt for other lipid-hydrophilic polypeptide complexes. For example, in a behenic acid-polyarginine complex the hydrocarbon chains are oriented perpendicular to the plane of the bilayer (McIntosh, T.J. and Waldbillig, R.C., unpublished observation). It has been shown that divalent cations affect the hydrocarbon chain packing parameters [27]. Clearly head group interactions have a strong influence both on the ultrastructure of the bilayer hydrocarbon core and on the stability of the bilayer.

Acknowledgements

We wish to thank Dr. W. Longley for very helpful discussions during the course of our investigations. This work was supported by grants from the National Institutes of Health (Program Project Research grant 5 P01 NS 10299, Institutional Research Fellowship 1 T22 GM00100, and Individual Research Fellowship 1 F32 GM05149). Dr. Waldbillig was partially supported by a fellowship from the National Multiple Sclerosis Society.

References

- 1 Robertson, J.D. (1957) *J. Biophys. Biochem. Cytol.* 3, 1043–1048
- 2 Engstrom, A. and Finean, J.B. (1958) *Biological Ultrastructure* pp. 215–242, Academic Press, New York
- 3 Robertson, J.D. (1960) *Progress in Biophysics* 10, 343–418
- 4 Worthington, C.R. (1972) *Ann. N.Y. Acad. Sci.* 195, 293–308
- 5 Kirschner, D.A. and Caspar, D.L.D. (1972) *Ann. N.Y. Acad. Sci.* 195, 309–320
- 6 Bretscher, M.S. (1972) *J. Mol. Biol.* 71, 523–528
- 7 Gordeky, S.E. and Marinetti, G.V. (1973) *Biochem. Biophys. Res. Commun.* 50, 1027–1031
- 8 Verkleij, A.J., Zwaal, R.F.A., Roelofsen, B., Confurius, P., Kastelijn, D. and Van Deenen, L.L.M. (1973) *Biochim. Biophys. Acta* 323, 178–193
- 9 Zwaal, R.F.A., Roelofsen, B. and Colley, C.M. (1973) *Biochim. Biophys. Acta* 300, 159–182
- 10 Trams, E.G. and Lauter, C.J. (1974) *Biochim. Biophys. Acta* 345, 180–197
- 11 Whiteley, N.M. and Berg, H.C. (1974) *J. Mol. Biol.* 87, 541–561
- 12 Gordeky, S.E., Marinetti, G.V. and Love, R. (1975) *J. Membrane Biol.* 20, 111–132
- 13 Fisher, K.A. (1976) *Proc. Natl. Acad. Sci. U.S.* 73, 173–177
- 14 Bretscher, M.S. (1972) *Nat. New Biol.* 236, 11–12
- 15 Singer, S.J. (1974) in *Perspectives in Membrane Biology* (Estrade, S. and Githers, C., eds.), pp. 131–147, Academic Press, New York

- 16 Steck, T.L. (1974) *J. Cell Biol.* 62, 1—19
- 17 Mateu, L., Luzzati, V., London, Y., Gould, R.M., Vosseberg, F.G. and Olive, J. (1973) *J. Mol. Biol.* 75, 697—709
- 18 Montal, M. and Mueller, P. (1972) *Proc. Natl. Acad. Sci. U.S.* 69, 3561—3566
- 19 Montal, M. (1973) *Biochim. Biophys. Acta* 298, 750—754
- 20 Sherwood, D. and Montal, M. (1975) *Biophys. J.* 15, 417—433
- 21 Hall, J.E. and Latorre, R. (1976) *Biophys. J.* 16, 99—103
- 22 Tardieu, A., Luzzati, V. and Reman, F.C. (1973) *J. Mol. Biol.* 75, 711—733
- 23 Hitchcock, P.B., Mason, R. and Shipley, G.G. (1975) *J. Mol. Biol.* 94, 297—299
- 24 Zaccai, G., Blasie, J.K. and Schoenborn, B.P. (1975) *Proc. Natl. Acad. Sci. U.S.* 72, 376—380
- 25 Franks, N.P. (1976) *J. Mol. Biol.* 100, 345—358
- 26 Waldbillig, R.C., Robertson, J.D. and McIntosh, T.J. (1976) *Biochim. Biophys. Acta* 448, 1—14
- 27 McIntosh, T.J., Waldbillig, R.C. and Robertson, J.D. (1967) *Biochim. Biophys. Acta* 448, 15—33
- 28 Langmuir, I. (1920) *Trans. Faraday Soc.* 15, 62—69
- 29 Blodgett, K.B. (1935) *J. Am. Chem. Soc.* 57, 1007—1022
- 30 Deamer, D.W. and Branton, D. (1967) *Science* 158, 655—657
- 31 Schildovsky, G. (1965) *Lab. Invest.* 14, 475—495
- 32 Sato, J. (1968) *Jap. J. Elec. Micros.* 17, 158—159
- 33 Longley, W. and Miller, R. (1975) *Rev. Sci. Instrum.* 46, 30—32
- 34 Lesslauer, W. and Blasie, J.K. (1972) *Biophys. J.* 12, 175—190
- 35 Stallberg-Stenhagen, S. and Stenhagen, E. (1945) *Nature* 156, 239—240
- 36 Honig, E.P. (1973) *J. Coll. Interface Sci.* 43, 66—72
- 37 Honig, E.P., Hengst, J.M.Th. and den Engelsens, D. (1973) *J. Coll. Interface Sci.* 45, 92—102
- 38 Montal, M. (1972) *J. Membrane Biol.* 7, 245—266
- 39 Donnay, J.D.M. and Donnay, G. (1967) in *International Table for X-ray Crystallography* (Kasper, J.S. and Lonsdale, K., eds.), Vol. II, p. 107
- 40 Abrahamsson, S. and Von Sydow, E. (1954) *Acta Cryst.* 7, 591—592
- 41 Deamer, D.W., Meek, D.W. and Cornwell, D.G. (1967) *J. Lipid Res.* 8, 255—263
- 42 Glaeser, R.M. and Deamer, D.W. (1969) *Electron Microsc. Soc. Am. 27th Meeting*, p. 338
- 43 Baumeister, W., Fringeli, U.P., Hahn, M., Kopp, F. and Serdynski, J. (1976) *Biophys. J.* 16, 791—810
- 44 Gulik-Krzywicki, T. (1975) *Biochim. Biophys. Acta* 415, 1—28
- 45 Degerman, G. and von Sydow, E. (1958) *Acta Chem. Scand.* 12, 1176—1182
- 46 Podo, F. and Blasie, J.K. (1976) *Biochim. Biophys. Acta* 419, 1—18
- 47 Muramatsu, M. and Sasaki, T. (1952) *Bull. Chem. Soc. Japan* 25, 21—28
- 48 Ehlert, R.C. (1965) *J. Coll. Interface Sci.* 20, 387—390
- 49 Charles, M.W. (1971) *J. Appl. Phys.* 42, 3329—3356